DOI: 10.1002/chem.201102571

Molecular Recognition at the Active Site of Factor Xa: Cation–π Interactions, Stacking on Planar Peptide Surfaces, and Replacement of Structural Water

Laura M. Salonen,[a] Mareike C. Holland,[a] Philip S. J. Kaib,[a] Wolfgang Haap,*[b] Jörg Benz,[b] Jean-Luc Mary,[b] Olivier Kuster,[b] W. Bernd Schweizer,[a] David W. Banner,[b] and François Diederich*[a]

Abstract: Factor Xa, a serine protease from the blood coagulation cascade, is an ideal enzyme for molecular recognition studies, as its active site is highly shape-persistent and features distinct, concave sub-pockets. We developed a family of non-peptidic, small-molecule inhibitors with a central tricyclic core orienting a neutral heterocyclic substituent into the S1 pocket and a quaternary ammonium ion into the aromatic box in the S4 pocket. The substituents were systematically varied to investigate cation–π interactions in the S4 pocket, optimal heterocyclic stacking on the flat peptide walls lining the S1 pocket, and potential water replacements in both the S1 and the S4 pockets. Structure–activity relationships were established to reveal and quantify contributions to the binding free enthalpy, resulting from single-atom replacements or positional changes in the ligands. A series of high-affinity ligands with inhibitory constants down to K_i = 2 nM were obtained and their proposed binding geometries confirmed by X-ray co-crystal structures of protein–ligand complexes.

Keywords: cation–π interactions · enzyme inhibitors · factor Xa · ligand conformations · molecular recognition

Introduction

We decipher and quantify protein–ligand interactions at the level of individual atoms in an approach comprising structure-based design and synthesis of non-peptidic, small-molecule enzyme inhibitors, analysis of their biological affinities, and X-ray crystallography of protein–ligand co-crystal structures. The resulting insight into molecular recognition processes is not only useful in the development and optimization of active compounds in the pharmaceutical and crop protection industry, but also in many other areas of chemical research, such as supramolecular chemistry and catalyst development.

Previously, we identified the enzyme factor Xa, a serine protease from the human blood coagulation cascade,[1] as an excellent model system for molecular recognition studies.[2] Its active site is highly shape-persistent and features distinct, concave sub-pockets. As a central enzyme in the blood coagulation cascade, factor Xa cleaves prothrombin to form thrombin initiating the common pathway, which ultimately leads to the formation of fibrin clots. The pharmaceutical industry has undertaken large efforts in the development of direct factor Xa inhibitors as new antithrombotic agents,[3] and the first drug rivaroxaban (Xarelto)[3f] has received market approval.

Factor Xa inhibitors are typically L-shaped, with a central core orienting the virtually orthogonal S1 and S4 vectors to their respective pockets (Figure 1). The active site of factor Xa is located mainly on the surface of the enzyme, except for the S1 binding pocket, which reaches towards the core with Asp189 and Tyr228 at the bottom. This pocket was

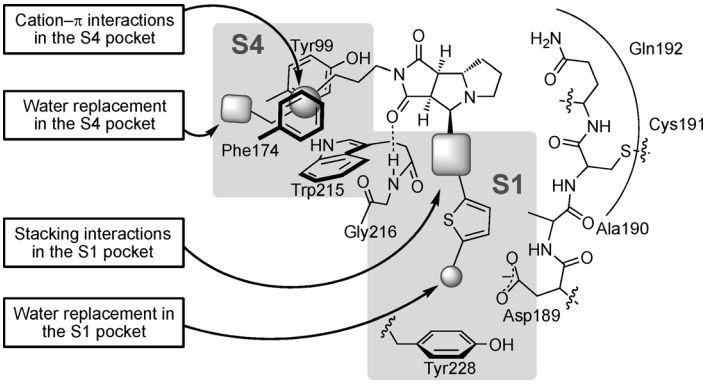

Figure 1. Schematic representation of the active site of factor Xa and ligand design.

[a] L. M. Salonen, M. C. Holland, P. S. J. Kaib, Dr. W. B. Schweizer, Prof. Dr. F. Diederich
Laboratorium für Organische Chemie
ETH Zürich
Wolfgang-Pauli-Strasse 10, HCI, 8093 Zürich (Switzerland)
Fax: (+41) 44-632-1109
E-mail: diederich@org.chem.ethz.ch

[b] Dr. W. Haap, Dr. J. Benz, J.-L. Mary, O. Kuster, Dr. D. W. Banner
Pharma Division
Präklinische Forschung
F. Hoffmann-La Roche AG
4070 Basel (Switzerland)
E-mail: wolfgang.haap@roche.com

Supporting information for this article is available on the WWW under http://dx.doi.org/10.1002/chem.201102571.

filled in earlier inhibitor development with cationic phenylamidinium substituents interacting with the anionic side chain of Asp189, thereby mimicking the interaction of Asp189 with the side chain of Arg in the complex of the natural substrate prothrombin.[3d] Currently, the more favored approach is targeting the S1 pocket with halogenated arenes and heteroarenes, with the halide substituent approaching the side chain of Tyr228 at the bottom of the pocket, which ultimately enabled the discovery of drug-like compounds.[3]

The other main binding pocket, the S4 pocket, is shaped by the side chains of Tyr99, Phe174, and Trp215. This "aromatic box" is an attractive site to study cation–π interactions.[4] One of our earlier inhibitors featuring a tricyclic core similar to the one in the new ligands, binding to the S4 pocket with a quaternary ammonium moiety (Me_3N^+-, see Figure 1SI in the Supporting Information) and to the S1 pocket with a phenylamidinium substituent ("needle"), was active against factor Xa with an inhibitory constant K_i = 280 nM, whereas its neutral *tert*-butyl (Me_3C-) counterpart binds only weakly (K_i = 29 μM). This single-atom replacement (N^+/C) allowed the quantification of cation–π interactions in the S4 pocket as $\Delta\Delta G_{C\rightarrow N+} = -2.8$ kcal mol^{-1}.[2a] When the phenylamidinium needle was replaced with an isoxazolyl-chlorothienyl moiety ((±)-**1**, Scheme 1),[2b] the onium ion ligand was bound much more strongly with K_i = 9 nM, whereas the *tert*-butyl derivative (±)-**2** gave K_i = 550 nM ($\Delta\Delta G_{C\rightarrow N+} = -2.5$ kcal mol^{-1}, about -0.8 kcal mol^{-1} per aromatic ring lining the aromatic box).

Here, we provide further insight into the strength of cation–π interactions in the S4 pocket at the active site of factor Xa. Additionally, we identify a chain of conserved water molecules at the back of the S4 pocket, as seen in the X-ray co-crystal structures, and present our first approaches to replace these by ligand parts. In the S1 pocket, we probe the stacking interactions of the ligand with the flat peptide backbone segments lining the pocket and address the role of the chlorine substituent approaching the side chain of Tyr228.

Results and Discussion

Cation–π interactions: We previously reported the X-ray co-crystal structure of (±)-**1** with factor Xa (PDB code: 2JKH, 1.25 Å resolution; Figure 1SI),[2b] which shows the 3a*S*,4*R*,8a*S*,8b*R*-configured enantiomer bound at the active site as predicted by molecular modeling (Moloc).[5] The quaternary ammonium ion sits in the center of the aromatic box in a very similar manner to that seen in the X-ray co-crystal structure of the phenylamidinium inhibitor with factor Xa (PDB code: 2BOK, 1.64 Å resolution; Figure 1SI).[2a] However, the position of the tricyclic core of the inhibitor changes drastically shifting from the back (phenylamidinium) to the front ((±)-**1**) of the active site (Figure 1SI). The heterobiaryl needle in (±)-**1** undergoes efficient π-stacking interactions with the highly polar walls of the S1 pocket, and the Cl atom is directed towards Tyr228 (see below).

We first undertook the optical resolution of (±)-**1** to verify which of the (+)- or (−)-enantiomers corresponds to the 3a*S*,4*R*,8a*S*,8b*R*-configured one bound at the active site of factor Xa in the X-ray co-crystal structure of (±)-**1**, and to determine the degree of enantioselectivity of the binding process. The *endo,trans*-configured[2] racemate (±)-**3** is one of four possible diastereoisomeric pairs of enantiomers formed in the 1,3-dipolar cycloaddition between maleinimide **4**, L-proline (**5**), and aldehyde **6** (Scheme 1).[6] It can be isolated by rather tedious column chromatography (SiO_2).

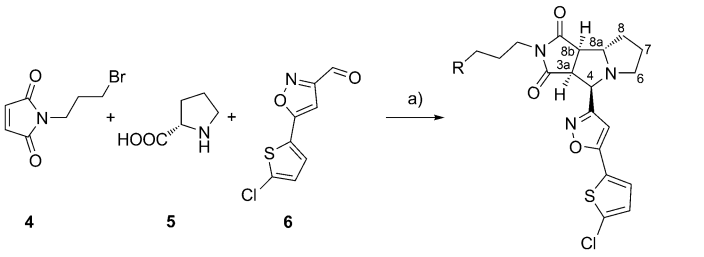

Compound	R	K_i / nM
(±)-**1**	$Me_3N^+Br^-$	9
(±)-**2**	Me_3C	550
(+)-**1**	$Me_3N^+Br^-$	5
(−)-**1**	$Me_3N^+Br^-$	271
(±)-**7**	$Me_3P^+Br^-$	7
(±)-**14**	$Me_3N^+I^-$	18

b) (±)-**3** R = Br; (±)-**1** R = $Me_3N^+Br^-$

Scheme 1. Synthesis and biological activities of new inhibitors of factor Xa. Compounds (±)-**1** and (±)-**2** have been previously reported.[2b] a) MeCN, 80 °C, 24 h, 4%; b) Me_3N (4.2 M in EtOH), EtOH, RT, 46 h, 93%. Inhibitory constants are averages of 1–3 duplicate measurements.

Enantiomeric resolution of (±)-**3** was achieved by HPLC on a chiral stationary phase (Chiralpak AD), and the enantiomers were subsequently converted in excellent yield into the trimethylammonium derivatives (+)-**1** and (−)-**1** by reaction with Me_3N. The enantiomers were tested for their biological activity towards factor Xa in a spectrophotometric assay,[7] and for selectivity against thrombin[8] (for description of the assays and thrombin binding data, see the Supporting Information). Enantiomer (+)-**1** (K_i = 5 nM) has an approximately 50-fold higher affinity towards factor Xa than (−)-**1** (K_i = 271 nM), and consequently, we can unambiguously assign the absolute configuration of (+)-**1** as 3a*S*,4*R*,8a*S*,8b*R*.

Next, we prepared the trimethylphosphonium derivative (±)-**7** by treating (±)-**3** with a solution of Me_3P in THF. We found that (±)-**7** binds to factor Xa with K_i = 7 nM (Scheme 1), in a similar range of activity to trimethylammonium derivative (±)-**1**. Thus, the change in the nature and the size of the cation does not significantly affect the binding affinity. Such results have been reported in the literature for resorcinarene and pyrogallolarene cavitands, where the

larger tetramethylphosphonium cation (115 Å^3) was bound with a similar association constant to that of the tetramethylammonium guest (105 Å^3) in the aromatic cavity.[9]

In the previous study,[2b] we prepared primary, secondary, and tertiary amines (±)-**8**–(±)-**10** (Figure 2), which are fully protonated under the conditions of the biological assay at pH 7.8, and found the degree of methylation to have a dramatic effect on the strength of the cation–π interaction, with a stepwise energetic gain ($-\Delta\Delta G$) of 1.2–1.8 kcal mol^{-1} per methylation. We now synthesized the neutral, alkyl-bearing ligands (±)-**11**-(±)-**13** to function, in addition to (±)-**2**,[2b] as control compounds (Figure 2; for synthetic procedures, see the Supporting Information). It should be noted that the compounds in this neutral series have low water-solubility, which results in substantial uncertainties in their experimentally determined binding activities.

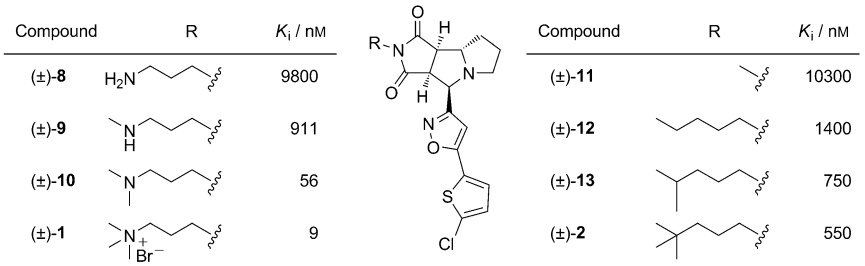

Figure 2. Biological activities of the ammonium ion series (±)-**8**–(±)-**10**, which are all fully protonated under the conditions of the assay at pH 7.8, quaternary ammonium (±)-**1**, and control compounds (±)-**11**–(±)-**13** and (±)-**2**. All inhibitory constants are averages of 1–3 duplicate measurements. Due to solubility problems in the case of the neutral (±)-**11**–(±)-**13** and (±)-**2**, the measurements have large uncertainties.

An enormous loss in binding affinity was observed when the S4 vector was entirely omitted: *N*-methyl ligand (±)-**11** binds with $K_i = 10.3$ μM, showing that occupying the S4 pocket is crucial to maintain the high activity of the inhibitors. Activity increases by a factor of ten with the incorporation of an *n*-pentyl vector as in (±)-**12** ($K_i = 1.4$ μM). Slight enhancements in affinity are observed with additional methyl groups, with the 4-methylpentyl-bearing ligand (±)-**13** binding with $K_i = 0.75$ μM, and finally the 4,4-dimethylpentyl ("*tert*-butyl") derivative (±)-**2** with $K_i = 0.55$ μM. The binding affinity is enhanced by approximately a factor of three when moving from the *n*-pentyl to the 4,4-dimethylpentyl derivative. In sharp contrast, binding affinity increases by a factor of 1000 when moving from the primary (K_i = 9.8 μM) to the quaternary ammonium ion inhibitor (K_i = 9 nM), corroborating the increasingly strong cation–π interaction in that series (Figure 2).

Counteranion effects on cation–π interactions have been investigated with model systems in organic solvents.[10] To address potential counteranion effects in the binding of the quaternary ammonium ion inhibitors to factor Xa, we prepared iodide (±)-**14** (Scheme 1) by a Finkelstein reaction of (±)-**3** with NaI and subsequent treatment of the product with Me_3N. The inhibitory constant for iodide (±)-**14** was determined to be $K_i = 18$ nM, in a similar range to that of bromide (±)-**1**. Thus, in our system, exchanging the counteranion seems to have a negligible influence on the strength of the cation–π interaction under the conditions of the assay (buffer solution at pH 7.8). As the aromatic box is open towards the surface of the protein, we presume that the onium salts bind as solvent-separated ion pairs.

Water replacement in the S1 pocket: In the X-ray co-crystal structure of (±)-**1** bound to factor Xa, the Cl atom on the thienyl ring is directed towards Tyr228 in the S1 pocket (d(Cl···C-OH) = 3.6 Å, angle (Cl···C-O) = 82°) and undergoes van der Waals interactions with the surrounding amino acids Ala190, Val213, Gly226, and Ile227 (d(Cl···C/N) = 3.5–3.8 Å) (Figure 2SI). In a search of the Protein Data Bank (PDB) using Relibase,[11] we found the location of the Cl atom and its approach angle to the phenol ring to be highly conserved among the X-ray co-crystal structures of factor Xa inhibitors.[2b,12] We believe that the position of the Cl atom in the co-crystal structures of factor Xa ligands with terminally chlorinated S1 needles reflects favorable dipolar interactions with the phenolic C–O dipole[13] while avoiding close Cl···π contacts.[12] Remarkably, the specific position of the Cl atom closely resembles that of a structural water molecule seen in both the co-crystal structure of the earlier phenylamidinium inhibitor (PDB code: 2BOK; for overlay, see Figure 1SI)[14] and the X-ray crystal structure of factor Xa without a bound ligand (resolution 2.2 Å, PDB code: 1HCG).[1] In the phenylamidinium structure, this water molecule undergoes dipolar interactions with the C–O dipole of the phenolic ring of Tyr228 (d(O···C-OH) = 3.4 Å, angle (O···C-O) = 115°) and hydrogen bonding to Ile227 (d(C=O···(H)OH) = 2.9 Å) and to the phenylamidinium S1 needle of the inhibitor (d-(N···(H)OH) = 3.1 Å). We therefore propose that the Cl substituent in (±)-**1** displaces this water[15] and substitutes the dipolar interaction with the phenolic C–O(H) group, while undergoing favorable van der Waals interactions with the surrounding lipophilic amino acid residues. The replacement of conserved water molecules seen in X-ray co-crystal structures of protein–ligand complexes is of substantial interest in contemporary structure-based drug design.[16]

We prepared a series of compounds with different thienyl substituents ((±)-**15**-(±)-**19**, Figure 3, for synthesis, see the Supporting Information) and studied their biological activity.[17] The Cl atom indeed makes a large contribution to the binding free enthalpy of (±)-**1**. Substitution of Cl by H ((±)-**15**) increases the inhibitory constant by a factor of 70 to $K_i = 612$ nM, corresponding to a loss of binding free

Compound	R	K_i / nM
(±)-**15**	H	612
(+)-**16**	OMe	509
(−)-**16**	OMe	3540
(±)-**17**	F	48
(±)-**1**	Cl	9
(±)-**18**	Br	6
(±)-**19**	I	47

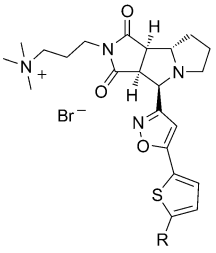

Figure 3. Influence of thienyl ring substituents on binding affinity. Inhibitory constants are averages of 1–3 duplicate measurements.

Compound	Het	K_i / nM
(±)-**1**		9
(±)-**20**		146
(±)-**21**		1620

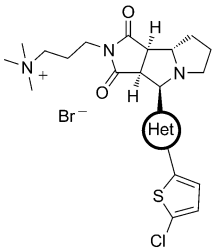

Figure 4. Influence of heteroatom positions in the S1 needle on binding affinity. Inhibitory constants are averages of 2–3 duplicate measurements.

enthalpy of $\Delta\Delta G = 2.6$ kcal mol^{-1}, in agreement with reports in the literature.[12] While the brominated ligand (±)-**18** ($K_i = 6$ nM) is of similar potency to (±)-**1**, the iodine substituent in (±)-**19** seems to be too large and affinity drops by nearly an order of magnitude ($K_i = 47$ nM). The same reduction in binding is measured for fluorinated (±)-**17** ($K_i = 48$ nM), presumably as a result of the unfavorable proximity of the F atom to the phenolic π-surface of Tyr228,[18] and less favorable van der Waals contacts due to the smaller size of the F atom compared to the larger organohalogens.[19] These unfavorable effects seem to overcompensate the stronger dipolar interaction with the phenolic C–O, expected for the C–F bond. A large loss in affinity is observed for the methoxy-substituted ligands ((+)-**16**: $K_i = 509$ nM, (−)-**16**: $K_i = 3540$ nM). The methoxy group is presumably unable to interact with Tyr228 in a favorable geometry, thus resulting in a loss of binding affinity. Additionally, a higher desolvation penalty as compared to the iodinated analogue, for example, may play a role. However, a different binding mode, with the MeO substituent pointing to Asp189 at the bottom of the S1 pocket, as reported in the literature,[3a] cannot be excluded in this case.

Stacking on planar peptide backbone fragments in the S1 pocket: Backbone planar peptides line the walls of the narrow S1 pocket, Ala190-Cys191-Gln192 on one side, and Trp215-Gly216 on the other (Figure 1). The X-ray co-crystal structure of (±)-**1** with factor Xa showed that these backbone surfaces undergo stacking interactions at van der Waals distance with the isoxazolyl-chlorothienyl needle (see Figure 3SI).[2b] To investigate these interactions in greater detail, we alternated the positions of the heteroatoms on the isoxazole ring of (±)-**1** and prepared the oxazole-containing ligands (±)-**20** and (±)-**21** (Figure 4; for synthesis, see the Supporting Information). The compounds were tested for their biological activity and, to our great surprise, were found to be much weaker factor Xa inhibitors than (±)-**1**, with a K_i value of 146 nM for (±)-**20** and $K_i = 1620$ nM for (±)-**21**.

To clarify the reasons for this large loss in activity when replacing the isoxazole with an oxazole ring, we obtained X-ray co-crystal structures of both (±)-**20** and (±)-**21** in complex with factor Xa (Figure 5; PDB code: 2Y5G for (±)-**20** at 1.33 Å resolution and 2Y5H for (±)-**21** at 1.29 Å resolution). An overlay of the three co-crystal structures of (±)-**1**, (±)-**20**, and (±)-**21** is shown in Figure 6. The active

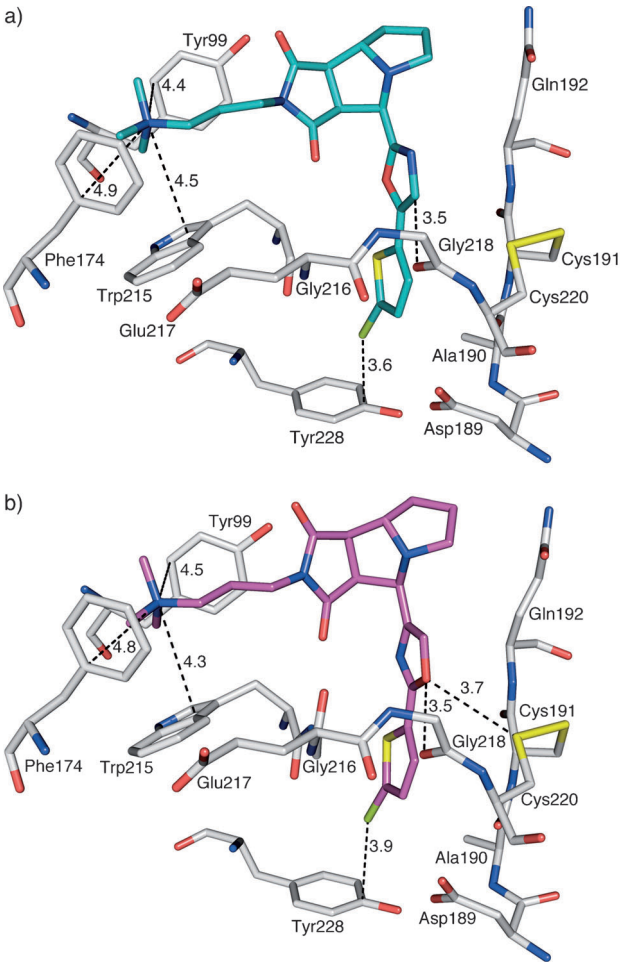

Figure 5. X-ray co-crystal structures of inhibitors a) (±)-**20** (turquoise) and b) (±)-**21** (magenta) bound at the active site of factor Xa (PDB codes: 2Y5G and 2Y5H, resolutions 1.33 Å and 1.29 Å, respectively). Distances are shown in Å. Color code: gray C_{enzyme}, turquoise $C_{(\pm)\text{-}20}$, magenta $C_{(\pm)\text{-}21}$, red O, blue N, yellow S, lime Cl.

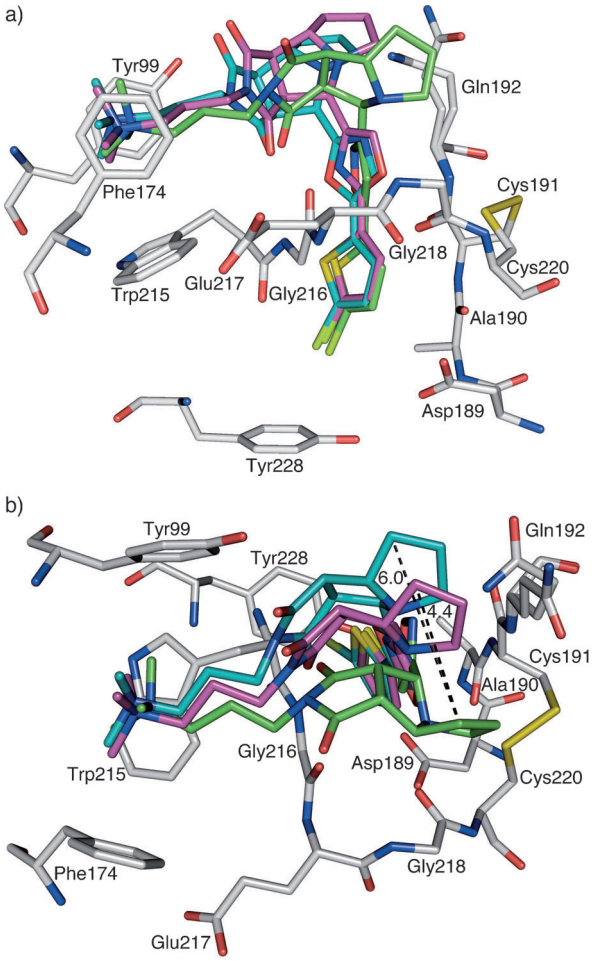

Figure 6. Overlay of inhibitors (±)-**1** (green), (±)-**20** (turquoise), and (±)-**21** (magenta) bound at the active site of factor Xa (PDB codes: 2JKH, 2Y5G, and 2Y5H, respectively). Only the enzyme of 2JKH is shown. a) View onto the entire inhibitor. b) View from the top on the tricyclic core. Color code: gray C_{enzyme}, green $C_{(\pm)\text{-}1}$, turquoise $C_{(\pm)\text{-}20}$, magenta $C_{(\pm)\text{-}21}$, red O, blue N, yellow S, lime Cl.

site of the enzyme is completely conserved in all three structures (Figure 4SI). In all three complexes, the key binding interactions are fully established: the onium ion is located in the center of the S4 pocket, and the chlorothienyl needle undergoes favorable interactions at the bottom of the S1 pocket. The van der Waals contacts between the Cl atom and the surrounding amino acids are in the same range in each case. The thiophene ring stacks at a similar distance onto Gly216-Trp215 in all three structures (see Figure 3SI, 6SI, 7SI) and the Cl atom is positioned in a similar manner (d(Cl···C-O=3.6 Å, 3.6 Å, and 3.9 Å and angle Cl···C-O = 82°, 86°, and 86° for (±)-**1**, (±)-**20**, and (±)-**21**, respectively). The small displacement of the Cl atom in (±)-**21** away from Tyr228 can account for some of the loss in activity as suggested in the literature,[20] but this is clearly not the sole reason.

Figure 6 shows that the overall binding conformation of the inhibitors is different for (±)-**20** and (±)-**21** as compared to (±)-**1**: the oxazole ring in both ligands has flipped relative to the isoxazole ring of (±)-**1**. This flip apparently induces the tricyclic core to shift to the back of the active site, with its location now resembling more closely that of the earlier phenylamidinium inhibitor bound to factor Xa (PDB code: 2BOK, see Figure 1SI). Significant differences in the contacts of the tricyclic core with the protein are, however, not apparent in the different geometries, as the core resides in a spacious part of the active site, open to the surface.

The strongly reduced affinity and the different conformation of bound (±)-**20** and (±)-**21**, as compared to (±)-**1**, must originate from the interplay of several factors, which taken alone cannot fully explain the experimental findings.

i) Gas-phase conformational analysis (DFT B3LYP/6-311G(d,p)) of the free ligands showed that in the global minimum of free (±)-**1**, the isoxazole ring adopts the same alignment with respect to the tricyclic core as seen in the X-ray co-crystal structure. The energetic minimum with a flipped geometry is found higher in energy by up to 2.9 kcal mol^{-1}, presumably due to lone-pair repulsion between the tricyclic amine center and the isoxazole N atom. In the medium-strength ligand (±)-**20**, minima for both orientations of the oxazole ring are observed within 1 kcal mol^{-1}. The analysis of the weakly binding compound (±)-**21** shows a clear preference for the flipped geometry, as the lone pair of the tricyclic amine N atom interacts favorably with a C–H moiety of the oxazole ring. The flipping of the oxazole ring as compared to the isoxazole ring is, therefore, partially a result of the intrinsic conformational preferences of ligands (±)-**20** and (±)-**21**. When the various energetic minima geometries of the three ligands, identified in the conformational search, were docked into the active site, the key binding interactions of both the onium ion and the chlorothienyl moiety were only established properly when the conformers resembling those seen in the X-ray co-crystal structures were docked in and positioned as seen experimentally. In other words, the tricyclic core in (±)-**20** and (±)-**21** apparently needs to change position to efficiently establish these key contacts.

ii) Another relevant matter may be the surprisingly different angle between the two bonds departing from the isoxazole in (±)-**1** and from the oxazole rings in (±)-**20** and (±)-**21**. A CSD search (Figure 8SI) showed that the angle in 3,5-disubstituted isoxazoles varies from 153° to 162°, with a predominance around 157°. In contrast, the angles in the two oxazoles are much smaller. The angle in 2,4-disubstituted oxazoles, as in (±)-**20**, varies between 127° and 137°, with a maximum of occurrences around 130°, whereas in 2,5-disubstituted oxazoles as in (±)-**21** it varies between 132° and 152°, with a preference for 145–149°. In the co-crystal structures, the angle for the isoxazole ring in (±)-**1** is 147°, 133° for the oxazole ring in (±)-**20**, and 147° for the oxazole ring in (±)-**21**.

iii) The oxazole rings in (±)-**20** and (±)-**21** are nearly coplanar with the neighboring thiophene ring, whereas the

isoxazole ring of (±)-**1** is twisted by approximately 30° out of this plane (Figure 5SI). In the structure of (±)-**21**, a repulsive electrostatic contact between the O atom of the oxazole ring and the carbonyl O atom of Gly218 is established, (d(O···O=C–Gly218) = 3.5 Å, Figure 5b). As a result of the twist out of the thienyl plane, the isoxazole ring of (±)-**1** (Figure 3SI) establishes more favorable contacts to Gln192 than the oxazole rings in (±)-**20** (Figure 6SI) or (±)-**21** (Figure 7SI), with closest contacts between heavy atoms of d((is)oxazole···Gln192) = 3.3 ((±)-**1**), 3.8 ((±)-**20**), and 3.7 ((±)-**21**) Å, respectively.

iv) The positions of positively (δ^+) and negatively (δ^-) polarized atoms in the heterocycles are shifted when replacing the isoxazole ring with either of the oxazoles. This may affect the stacking interaction between the heterocycle and the flat polarizable peptide surfaces lining the S1 pocket, with their distinct δ^+ and δ^- centers. The importance of properly aligning centers of opposite polarity on stacking interactions has been clearly established in model systems.[21] Examination of the co-crystal structures shows that complementary intermolecular $\delta^+\cdots\delta^-$ contacts are best established by the isoxazole ring in (±)-**1**. This observation is certainly worth validating in further systematic study involving heterocyclic S1 needles with differently polarized frameworks.

Opportunities for water replacement at the back of the S4 pocket: When superimposing the X-ray co-crystal structures of (±)-**1**, (±)-**20**, and (±)-**21**, we identified a conserved chain of five water molecules located at the back of the S4 pocket (Figure 7). The water molecules are hydrogen-bonded to each other and the surrounding amino acids Ser173, Ile175, Glu97, and Thr98 (Figure 9SI, d(O(H)···(H)O/N) = 2.7–2.9 Å). Aiming at the replacement of one or more of these water molecules, a methyl group of the onium ion moiety of inhibitor (±)-**1** was exchanged for a H-bond-donating substituent (Figure 8). We envisioned a hydroxyl or amido group as first target vectors, and according to modeling with Moloc,[5] the hydrogen-bond donor of the inhibitors extends to the back of the aromatic box replacing a water molecule.

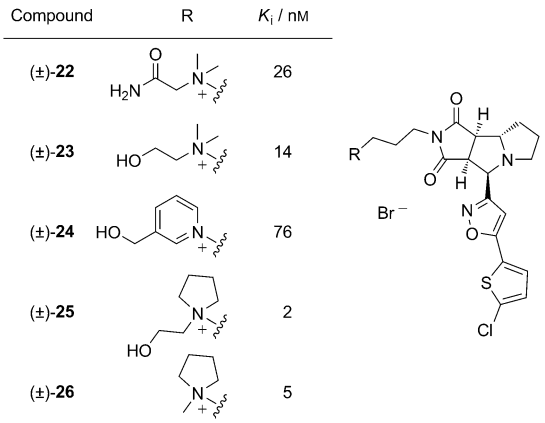

Figure 8. Inhibitors with polar groups departing from the onium ion. All inhibitory constants are averages of 1–4 duplicate measurements.

We prepared compounds (±)-**22**–(±)-**25** bearing substituents for potential water replacement (Figure 8; for inhibitor synthesis, see the Supporting Information). Ligand (±)-**22** (K_i = 26 nM) with an amide functionality is a weaker inhibitor of factor Xa than (±)-**1**. Likewise, inhibitors (±)-**23** and (±)-**24** (K_i = 14 nM and 76 nM, respectively) have lower binding affinities, also compared to the corresponding, previously reported ethyldimethylammonium- and pyridinium-bearing inhibitors, which lack the hydrogen bond-donating moieties (K_i = 8 and 30 nM, respectively).[2b] The loss of activity may be partly attributed to higher desolvation costs, as the inhibitors bearing the H-bond-donating residues are more hydrophilic than the corresponding control compounds. The X-ray crystal structure of the free ligand (±)-**24** was solved and revealed a homochiral dimeric assembly, in which the two molecules interact by forming two halogen bonds[22] between the chloro substituents on the thiophene rings and imide C=O groups (Figure 10SI).

The *N*-(2-hydroxyethyl)pyrrolidinium derivative (±)-**25** is our most potent factor Xa inhibitor to date with K_i = 2 nM. The high binding affinity was initially thought to stem from successful water replacement. We obtained the X-ray co-crystal structure of (±)-**25** in complex with factor Xa (Figure 9, PDB code: 2Y5F, resolution 1.29 Å), which shows the 3a*S*,4*R*,8a*S*,8b*R*-configured enantiomer bound at the active site in a binding mode resembling closely that of (±)-**1** (Figure 11SI). However, instead of reaching to the back of the S4 pocket to replace the first of the five water molecules of the chain, which remain conserved, the hydroxyethyl moiety is directed towards the surface of the protein and undergoes water-mediated hydrogen-bonding interactions to

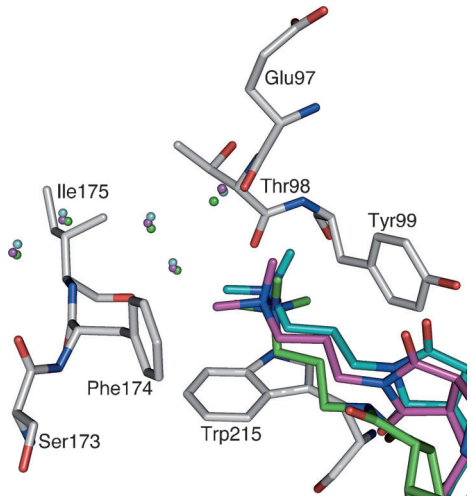

Figure 7. Conserved water molecules identified at the back of the S4 pocket. Only the enzyme of 2JKH is shown. Color code: gray C_{enzyme}, green $C_{(\pm)\text{-}1}$ and water, turquoise $C_{(\pm)\text{-}20}$ and water, magenta $C_{(\pm)\text{-}21}$ and water, red O, blue N.

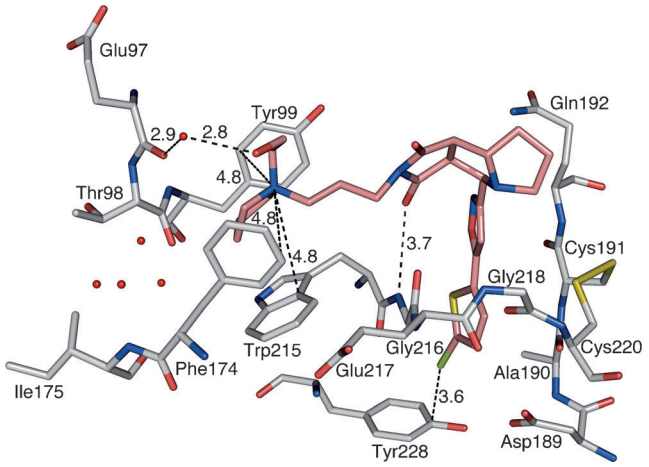

Figure 9. X-ray co-crystal structure of (±)-**25** bound at the active site of factor Xa (PDB code: 2Y5F, resolution 1.29 Å). Distances are shown in Å. Color code: gray C_{enzyme}, peach $C_{(\pm)\text{-}25}$, red O, blue N, yellow S, lime Cl.

the carbonyl of Glu97 ($d(H_2O\cdots(H)OCH_2$–(±)-**25**) = 2.8 Å; d(Glu97–C=O···(H)OH) = 2.9 Å). As a control, we prepared the *N*-methylpyrrolidinium ligand (±)-**26**, and determined its biological activity to be K_i = 5 nM. Evidently, the hydrogen-bonding interactions of (±)-**25** provide some additional stabilization to the complex, compensating for the increased desolvation costs due to the polar hydroxyethyl chain.

These results clearly show that the hydroxyethyl chain is too flexible for a water-replacement vector and that conformationally more rigidly positioned polar substituents, such as those of spirocyclic quaternary ammonium ions, will be required to accomplish the displacement of one or more of the conserved water molecules in the chain at the back of the S4 pocket.

Conclusion

This study confirms that potent inhibitors need to properly fill both the aromatic box in the S4 pocket and the S1 pocket of factor Xa. Quaternary ammonium ions are far superior substituents to fill the aromatic box than comparable alkyl substituents, with the single-atom ($N^+ \rightarrow C$) mutation strongly reducing binding affinity by up to $\Delta\Delta G_{N+\rightarrow C}$ = 2.5 kcal mol^{-1} as a result of the loss of cation–π interactions.

Optimal filling of the S1 pocket is challenging. The terminal chlorine substituent on the S1 needle must be properly positioned to undergo dipolar interactions with the phenol C–O(H) of Tyr228, to establish van der Waals contacts with neighboring lipophilic amino acid side chains, and to displace a water molecule interacting in a similar position with the phenolic ring in the absence of ligand.[1] The single-atom mutation on the thiophene ring (Cl → H) reduces binding affinity by $\Delta\Delta G_{Cl\rightarrow H}$ = 2.6 kcal mol^{-1}. In addition, the heterocyclic ring linking the tricyclic ligand core with the chlorothienyl moiety requires proper positioning in the S1 pocket to undergo favorable stacking interactions with the flat peptide walls lining the pocket and to generate optimal intermolecular interactions between oppositely polarized (δ^+ and δ^-) centers. The change in the overall binding geometry from the complex of (±)-**1** to the complexes of (±)-**20** and (±)-**21** is quite remarkable when merely substituting an isoxazole by oxazole rings. While replacements of one or more of the five conserved water molecules at the back of the S4 pocket by polar ligand parts have so far not been successful, the crystallographic analysis has shown the way to accomplish such replacements in future work. Factor Xa is clearly an ideal enzyme for precise molecular recognition studies at atomic level resolution, as its active site is completely conserved in all co-crystal structures discussed here, a prerequisite for assigning incremental energetic changes to single-atom mutations. Thus, this study allows gaining knowledge that can ultimately be generally applied to structure-based drug and crop protection agent design, as well as to many other areas of supramolecular chemistry.

Experimental Section

X-ray co-crystal structure determinations: Crystals of short form factor Xa (Arg150Glu mutant) were produced and data measured as previously described,[15g] except that data were collected at the Swiss Light Source. Data were processed with XDS[23] and SADABS (obtained from Bruker AXS), and data reduction used the CCP4 package.[24] The structures were solved by using the isomorphous 2jkh.pdb as starting model. Model building of the ligand was performed with Moloc,[5] and structures were refined with cycles of Coot[25] and Refmac5.[26] Coordinates have been deposited at the Protein Data Bank with the PDB codes: 2Y5G ((±)-**20**), 2Y5H ((±)-**21**), and 2Y5F ((±)-**25**). For more details, see the Supporting Information.

General details and synthetic procedures: In the following, the experimental details for the syntheses of compounds (+)-**1** and (−)-**1**, (±)-**7**, (±)-**20**, (±)-**21**, and (±)-**22**–(±)-**25** are described. All other synthetic details and experimental data are given in full in the Supporting Information. CC = column chromatography; RT = room temperature.

3-[(3a*S*,4*R*,8a*S*,8b*R*)-4-[5-(5-Chloro-2-thienyl)-1,2-oxazol-3-yl]-1,3-dioxo-octahydrodipyrrolo[1,2-*a*:3′,4′-*c*]pyrrol-2(3*H*)-yl]-*N*,*N*,*N*-trimethyl-1-propanaminium bromide ((+)-1): To a mixture of (+)-**3** (20 mg, 0.04 mmol) in EtOH (1 mL) at RT, 4.2 M Me_3N in EtOH (200 μL, 0.83 mmol) was added. The mixture was stirred at RT for 46 h and evaporated in vacuo. The residue was dissolved in MeOH. Precipitation from Et_2O gave (+)-**1** (20 mg, 89%) as off-white crystals. M.p. 214 °C (decomp); $[\alpha]_D^{25}$: +141.2 (c = 1, CH_3OH); ^{1}H NMR (600 MHz, CD_3OD): δ = 1.80–1.89 (m, 2H, H-C(7), H-C(8)), 2.01–2.09 (m, 2H, $^+NCH_2CH_2$), 2.11–2.19 (m, 2H, H-C(7), H-C(8)), 2.87 (ddd, J = 12.7, 8.3, 4.3 Hz, 1H, H-C(6)), 2.97 (ddd, J = 12.6, 8.7, 6.9 Hz, 1H, H-C(6)), 3.15 (s, 9H, $(CH_3)_3{}^+N$), 3.34–3.36 (m, 2H, $^+NCH_2$), 3.49 (dd, J = 8.1, 1.5 Hz, 1H, H-C(8b)), 3.56 (qt, J = 14.9, 6.5 Hz, 2H, $^+NCH_2CH_2CH_2$), 3.73–3.76 (m, 1H, H-C(8a)), 3.84 (t, J = 8.5 Hz, 1H, H-C(3a)), 4.43 (d, J = 8.8 Hz, 1H, H-C(4)), 6.63 (s, 1H, Ar), 7.11 (d, J = 4.0 Hz, 1H, Ar), 7.42 ppm (d, J = 4.0 Hz, 1H, Ar); ^{13}C NMR (150 MHz, CD_3OD): δ = 22.8, 24.2, 30.2, 36.7, 50.6, 50.8, 52.4, 53.6 (t), 62.7, 65.3 (t), 69.6, 101.4, 128.1, 129.0, 129.1, 134.2, 164.8, 165.1, 177.4, 179.9 ppm; IR (ATR): $\tilde{\nu}$ = 3386 (b), 2957, 1772, 1694, 1614, 1524, 1476, 1423, 1402, 1351, 1319, 1283, 1183, 1146, 1067, 1030, 1000, 965, 923, 878, 793, 751, 666, 628 cm^{-1}; HR-MALDI-MS: m/z (%): 465.1536 (42), $[M-Br]^+$, calcd for $C_{22}H_{28}{}^{37}ClN_4O_3S^+$: 465.1537, 463.1570 (100), $[M-Br]^+$, calcd for $C_{22}H_{28}{}^{35}ClN_4O_3S^+$: 463.1565.

3-[(3a*R*,4*S*,8a*R*,8b*S*)-4-[5-(5-Chloro-2-thienyl)-1,2-oxazol-3-yl]-1,3-dioxo-octahydrodipyrrolo[1,2-*a*:3′,4′-*c*]pyrrol-2(3*H*)-yl]-*N*,*N*,*N*-trimethyl-1-pro-

panaminium bromide ((−)-1): To a mixture of (−)-**3** (20 mg, 0.04 mmol) in EtOH (1 mL) at RT, 4.2 M Me_3N in EtOH (200 μL, 0.83 mmol) was added. The mixture was stirred at RT for 46 h and evaporated in vacuo. The residue was dissolved in MeOH. Precipitation from Et_2O gave (−)-**1** (21 mg, 94%) as off-white crystals. M.p. 214 °C (decomp); $[\alpha]_D^{25}$: −137.2 (c = 1, CH_3OH); ^{1}H NMR (600 MHz, CD_3OD): δ = 1.79–1.89 (m, 2H, H-C(7), H-C(8)), 2.02–2.09 (m, 2H, $^+NCH_2CH_2$), 2.11–2.19 (m, 2H, H-C(7), H-C(8)), 2.87 (ddd, J = 12.7, 8.4, 4.4 Hz, 1H, H-C(6)), 2.97 (ddd, J = 12.7, 8.7, 7.0 Hz, 1H, H-C(6)), 3.14 (s, 9H, $(CH_3)_3{}^+N$), 3.33–3.36 (m, 2H, $^+NCH_2$), 3.48 (dd, J = 8.1, 1.5 Hz, 1H, H-C(8b)), 3.56 (qt, J = 15.0, 6.5 Hz, 2H, $^+NCH_2CH_2CH_2$), 3.73–3.76 (m, 1H, H-C(8a)), 3.84 (t, J = 8.5 Hz, 1H, H-C(3a)), 4.42 (d, J = 8.8 Hz, 1H, H-C(4)), 6.63 (s, 1H, Ar), 7.10 (d, J = 4.0 Hz, 1H, Ar), 7.42 ppm (d, J = 3.9 Hz, 1H, Ar); ^{13}C NMR (150 MHz, CD_3OD): δ = 22.8, 24.2, 30.2, 36.7, 50.7, 50.8, 52.4, 53.7 (t), 62.7, 65.3 (t), 69.6, 101.4, 128.1, 129.0, 129.1, 134.2, 164.9, 165.1, 177.5, 179.9 ppm; IR (ATR): $\tilde{\nu}$ = 3385 (b), 2957, 1772, 1694, 1524, 1476, 1423, 1402, 1351, 1319, 1283, 1246, 1206, 1183, 1145, 1068, 1030, 1000, 965, 923, 898, 878, 794, 750, 665, 627 cm^{-1}; HR-MALDI-MS: m/z (%): 465.1528 (41), $[M-Br]^+$, calcd for $C_{22}H_{28}{}^{37}ClN_4O_3S^+$: 465.1537, 463.1562 (100), $[M-Br]^+$, calcd for $C_{22}H_{28}{}^{35}ClN_4O_3S^+$: 463.1565.

{3-[(3a*RS*,4*RS*,8a*SR*,8b*SR*)-4-[5-(5-Chloro-2-thienyl)-3-isoxazolyl]-1,3-dioxo-octahydrodipyrrolo[1,2-*a*:3′,4′-*c*]pyrrol-2(3*H*)-yl]propyl}-(trimethyl)phosphonium bromide ((±)-7): A mixture of 1 M Me_3P in THF (1.24 mL, 1.24 mmol) and (±)-**3** (30 mg, 0.06 mmol) was stirred at RT under N_2 for 16 h, treated with additional 1 M Me_3P in THF (1 mL, 1.00 mmol), and stirred for five days. The precipitate was filtered and washed with THF. The residue was dissolved in MeOH. Precipitation from Et_2O gave (±)-**7** (24 mg, 69%) as a white solid. M.p. 217 °C (decomp); ^{1}H NMR (400 MHz, CD_3OD): δ = 1.77–1.90 (m, 4H, H-C(7), H-C(8), $^+PCH_2CH_2$), 1.88 (d, 9H, J = 14.5 Hz, $(CH_3)_3P^+$) 2.10–2.25 (m, 4H, H-C(7), H-C(8), $^+PCH_2$), 2.86 (ddd, J = 12.4, 8.1, 4.3 Hz, 1H, H-C(6)), 2.97 (ddd, J = 12.6, 8.6, 6.9 Hz, 1H, H-C(6)), 3.49 (dd, J = 8.2, 1.5 Hz, 1H, H-C(8b)), 3.51–3.63 (m, 2H, $^+PCH_2CH_2CH_2$), 3.75 (br. t, J = 7.5 Hz, 1H, H-C(8a)), 3.84 (t, J = 8.5 Hz, 1H, H-C(3a)), 4.42 (d, J = 8.8 Hz, 1H, H-C(4)), 6.62 (s, 1H, Ar), 7.11 (d, J = 4.0 Hz, 1H, Ar), 7.42 ppm (d, J = 4.0 Hz, 1H, Ar); ^{13}C NMR (100 MHz, CD_3OD): δ = 7.7 (d, $^1J_{CP}$ = 55.1 Hz), 20.9 (d, $^2J_{CP}$ = 3.7 Hz), 21.6 (d, $^1J_{CP}$ = 54.1 Hz), 24.1, 30.2, 39.8 (d, $^3J_{CP}$ = 18.4 Hz), 50.65, 50.71, 52.4, 62.7, 69.6, 101.3, 128.1, 128.98, 129.02, 134.1, 164.9, 165.0, 177.4, 180.0 ppm; ^{31}P NMR (172 MHz, CD_3OD): δ = 28.0 ppm; IR (ATR): $\tilde{\nu}$ = 2956, 1769, 1694, 1604, 1527, 1475, 1424, 1398, 1370, 1336, 1306, 1280, 1245, 1203, 1159, 1103, 1063, 1029, 990, 973, 901, 873, 798, 768, 756, 727, 682, 667, 654, 623 cm^{-1}; HR-MALDI-MS: m/z (%): 482.1238 (39), $[M-Br]^+$, calcd for $C_{22}H_{28}{}^{37}ClN_3O_3PS^+$: 482.1248, 480.1272 (100), $[M-Br]^+$, calcd for $C_{22}H_{28}{}^{35}ClN_3O_3PS^+$: 480.1272.

3-[(3a*SR*,4*RS*,8a*SR*,8b*RS*)-4-[5-(5-Chloro-2-thienyl)-1,3-oxazol-2-yl]-1,3-dioxooctahydrodipyrrolo[1,2-*a*:3′,4′-*c*]pyrrol-2(3*H*)-yl]-*N*,*N*,*N*-trimethyl-1-propanaminium bromide ((±)-20): To a solution of (±)-**27** (17 mg, 0.04 mmol) in EtOH (2 mL) at RT was added 4.2 M Me_3N in EtOH (170 μL, 0.70 mmol). The mixture was stirred at RT for five days and evaporated in vacuo. The residue was dissolved in MeOH. Precipitation from Et_2O gave (±)-**20** (14 mg, 74%) as a yellow solid. M.p. 223 °C (decomp); ^{1}H NMR (600 MHz, $CDCl_3$): δ = 1.77–1.89 (m, 2H, H-C(7), H-C(8)), 2.01–2.08 (m, 2H, $^+NCH_2CH_2$), 2.10–2.19 (m, 2H, H-C(7), H-C(8)), 2.87 (ddd, J = 12.6, 8.2, 4.4 Hz, 1H, H-C(6)), 2.97–3.01 (m, 1H, H-C(6)), 3.13 (s, 9H, $(CH_3)_3{}^+N$), 3.33–3.37 (m, 2H, $^+NCH_2$), 3.49 (dd, J = 8.2, 1.5 Hz, 1H, H-C(8b)), 3.54–3.59 (m, 2H, $^+NCH_2CH_2CH_2$), 3.75 (ddd, J = 9.2, 7.3, 1.6 Hz, 1H, H-C(8a)), 3.91 (t, J = 8.5 Hz, 1H, H-C(3a)), 4.47 (d, J = 8.8 Hz, 1H, H-C(4)), 7.03 (d, J = 4.0 Hz, 1H, Ar), 7.22 (d, J = 3.9 Hz, 1H, Ar), 7.30 ppm (s, 1H, Ar); ^{13}C NMR (150 MHz, $CDCl_3$): δ = 22.7, 24.2, 30.4, 36.8, 50.5, 50.7, 52.4, 53.6 (t), 63.6, 65.2 (t), 69.6, 122.9, 125.4, 128.6, 129.5, 131.6, 147.9, 162.6, 177.5, 179.8 ppm; IR (ATR): $\tilde{\nu}$ = 2953, 1773, 1704, 1562, 1478, 1434, 1404, 1357, 1321, 1245, 1226, 1205, 1183, 1146, 1127, 1087, 1068, 1031, 960, 929, 884, 818, 777, 748, 668, 629 cm^{-1}; HR-MALDI-MS: m/z (%): 465.1531 (41), $[M-Br]^+$, calcd for $C_{22}H_{28}{}^{37}ClN_4O_3S^+$: 465.1537, 463.1567 (100), $[M-Br]^+$, calcd for $C_{22}H_{28}{}^{35}ClN_4O_3S^+$: 463.1565.

***N*,*N*,*N*-Trimethyl-3-[(3a*RS*,4*RS*,8a*SR*,8b*SR*)-4-[2-(5-Chloro-2-thienyl)-1,3-oxazol-4-yl]-1,3-dioxooctahydrodipyrrolo[1,2-*a*:3′,4′-*c*]pyrrol-2(3*H*)-yl]-1-propanaminium bromide ((±)-21)**: To (±)-**28** (12 mg, 0.02 mmol) in EtOH (0.25 mL) at RT, 4.2 M Me_3N in EtOH (120 μL, 0.5 mmol) was added. The mixture was stirred for six days at RT and the solvent evaporated in vacuo. The residue was dissolved in MeOH. Precipitation from Et_2O gave (±)-**21** (20 mg, quant.) as a white solid. M.p. 180 °C (decomp); ^{1}H NMR (600 MHz, $CDCl_3$): δ = 1.81–1.87 (m, 2H, H-C(7), H-C(8)), 1.99–2.08 (m, 2H, $^+NCH_2CH_2$), 2.09–2.18 (m, 2H, H-C(7), H-C(8)), 2.85–2.90 (m, 1H, H-C(6)), 2.94–2.98 (m, 1H, H-C(6)), 3.09 (s, 9H, $(CH_3)_3{}^+N$), 3.33–3.36 (m, 2H, $^+NCH_2$), 3.45–3.49 (m, 2H, H-C(8b), $^+NCH_2CH_2CH_2$), 3.56 (m, 1H, $^+NCH_2CH_2CH_2$), 3.79–3.82 (m, 2H, H-C(3a), H-C(8a)), 4.28 (d, J = 8.9 Hz, 1H, H-C(4)), 7.09 (d, J = 4.0 Hz, 1H, Ar), 7.51 (d, J = 4.0 Hz, 1H, Ar), 7.79 ppm (d, J = 0.7 Hz, 1H, Ar); ^{13}C NMR (150 MHz, $CDCl_3$): δ = 22.8, 24.3, 30.6, 36.8, 50.6, 51.1, 52.4, 53.6 (t), 62.6, 65.4 (t), 69.1, 128.9, 129.0, 129.4, 134.4, 137.9, 141.5, 158.0, 177.6, 180.1 ppm; IR (ATR): $\tilde{\nu}$ = 3383 (b), 2959, 1774, 1694, 1593, 1478, 1431, 1403, 1351, 1319, 1241, 1182, 1066, 1026, 982, 929, 906, 877, 803, 725, 663 cm^{-1}; HR-MALDI-MS: m/z (%): 465.1526 (33), $[M-Br]^+$, calcd for $C_{22}H_{28}{}^{37}ClN_4O_3S^+$: 465.1541, 463.1564 (100), $[M-Br]^+$, calcd for $C_{22}H_{28}{}^{35}ClN_4O_3S^+$: 463.1565.

***N*-(2-Amino-2-oxoethyl)-3-[(3a*RS*,4*RS*,8a*SR*,8b*SR*)-4-[5-(5-chloro-2-thienyl)-3-isoxazolyl]-1,3-dioxooctahydrodipyrrolo[1,2-*a*:3′,4′-*c*]pyrrol-2(3*H*)-yl]-*N*,*N*-dimethyl-1-propanaminium bromide ((±)-22)**: To a solution of (±)-**3** (23 mg, 0.05 mmol) in EtOH (1.5 mL) at RT, **29** (63 mg, 0.62 mmol) was added. The mixture was stirred at RT for three days and at 40 °C for four days. The mixture was evaporated in vacuo, dissolved in MeOH, and precipitation from Et_2O gave (±)-**22** (20 mg, 71%) as an off-white solid. M.p. 207 °C (decomp); ^{1}H NMR (600 MHz, $CDCl_3$): δ = 1.80–1.88 (m, 2H, H-C(7), H-C(8)), 2.02–2.09 (m, 2H, $^+NCH_2CH_2CH_2$), 2.11–2.19 (m, 2H, H-C(7), H-C(8)), 2.86 (ddd, J = 12.7, 8.4, 4.3 Hz, 1H, H-C(6)), 2.96 (ddd, J = 12.6, 8.6, 7.0 Hz, 1H, H-C(6)), 3.28 (s, 3H, CH_3), 3.30 (s, 3H, CH_3), 3.49 (dd, J = 8.1, 1.5 Hz, 1H, H-C(8b)), 3.52–3.63 (m, 4H, $^+NCH_2CH_2CH_2$, $^+NCH_2CH_2CH_2$), 3.74 (br. t, J = 7.7 Hz, 1H, H-C(8a)), 3.84 (t, J = 8.4 Hz, 1H, H-C(3a)), 4.07 (s, 2H, N^+CH_2CO), 4.41 (d, J = 8.7 Hz, 1H, H-C(4)), 6.64 (s, 1H, Ar), 7.11 (d, J = 4.0 Hz, 1H, Ar), 7.43 ppm (d, J = 4.0 Hz, 1H, Ar); ^{13}C NMR (150 MHz, $CDCl_3$): δ = 22.5, 24.2, 30.3, 36.6, 50.6, 50.8, 52.2, 52.5, 52.7, 62.5, 62.7, 64.3, 69.6, 101.2, 128.1, 129.0, 129.1, 134.2, 164.9, 165.1, 166.9, 177.5, 180.0 ppm; IR (ATR): $\tilde{\nu}$ = 3219, 3106, 2928, 1774, 1705, 1595, 1532, 1470, 1441, 1426, 1396, 1356, 1324, 1303, 1242, 1218, 1204, 1164, 1080, 1063, 1026, 997, 952, 907, 898, 871, 824, 789, 737, 667, 638, 609 cm^{-1}; HR-MALDI-MS: m/z (%): 506.1631 (100), $[M-Br]^+$, calcd for $C_{23}H_{29}{}^{35}ClN_5O_4S^+$: 506.1623.

3-[(3a*SR*,4*RS*,8a*SR*,8b*RS*)-4-[5-(5-Chloro-2-thienyl)-3-isoxazolyl]-1,3-dioxooctahydrodipyrrolo[1,2-*a*:3′,4′-*c*]pyrrol-2(3*H*)-yl]-*N*-(2-hydroxyethyl)-*N*,*N*-dimethyl-1-propanaminium bromide ((±)-23): To a solution of (±)-**3** (30 mg, 0.06 mmol) in EtOH (1 mL) at RT, *N*,*N*-dimethylethanolamine (125 μL, 1.24 mmol) was added and the mixture stirred at RT for 24 h and at 40 °C for further 24 h. The mixture was evaporated in vacuo. The residue was dissolved in MeOH. Precipitation from Et_2O gave (±)-**23** (26 mg, 73%) as a pink solid. M.p. 180 °C (decomp); ^{1}H NMR (600 MHz, CD_3OD): δ = 1.79–1.89 (m, 2H, H-C(7), H-C(8)), 2.00–2.07 (m, 1H, $^+NCH_2CH_2CH_2$), 2.09–2.19 (m, 3H, H-C(7), H-C(8), $^+NCH_2CH_2CH_2$), 2.96 (ddd, J = 12.7, 8.8, 7.0 Hz, 1H, H-C(6)), 2.87 (ddd, J = 12.7, 8.3, 4.3 Hz, 1H, H-C(6)), 3.16 (s, 3H, CH_3), 3.20 (s, 3H, CH_3), 3.34–3.61 (m, 7H, H-C(8b), $^+NCH_2CH_2CH_2$, $^+NCH_2CH_2CH_2$, CH_2CH_2OH), 3.70–3.73 (m, 1H, H-C(8a)), 3.84 (t, J = 8.4 Hz, 1H, H-C(3a)), 3.90–3.95 (m, 1H, CH_2OH), 4.12 (ddq, J = 14.0, 7.2, 2.4 Hz, 1H, CH_2OH), 4.44 (d, J = 8.8 Hz, 1H, H-C(4)), 6.66 (s, 1H, Ar), 7.11 (d, J = 4.0 Hz, 1H, Ar), 7.44 ppm (d, J = 3.8 Hz, 1H, Ar); ^{13}C NMR (150 MHz, CD_3OD): δ = 22.5, 24.1, 30.2, 36.6, 50.4, 50.7, 52.2, 52.5 (t), 52.6 (t), 56.8, 62.7, 63.9, 66.3, 69.5, 101.4, 128.1, 128.96, 129.02, 134.2, 164.7, 165.1, 177.4, 179.8 ppm; IR (ATR): $\tilde{\nu}$ = 3283, 3008, 2955, 2882, 1768, 1696, 1600, 1530, 1476, 1428, 1400, 1351, 1313, 1233, 1188, 1156, 1067, 1000, 963, 923, 895, 802, 742, 667, 632 cm^{-1}; HR-MALDI-MS: m/z (%): 495.1650 (37), $[M-Br]^+$, calcd for $C_{23}H_{30}{}^{37}ClN_4O_4S^+$: 495.1644, 493.1678 (100), $[M-Br]^+$, calcd for $C_{23}H_{30}{}^{35}ClN_4O_4S^+$: 493.1671; elemental analysis calcd (%) for $C_{23}H_{30}BrClN_4O_4S$ (572.09): C 48.13, H 5.27, N 9.76; found C 47.84, H 5.32, N 9.58.

1-{3-[(3a*SR*,4*RS*,8a*SR*,8b*RS*)-4-[5-(5-Chloro-2-thienyl)-3-isoxazolyl]-1,3-dioxooctahydrodipyrrolo[1,2-*a*:3′,4′-*c*]pyrrol-2(3*H*)-yl]propyl}-3-(hydroxymethyl)pyridinium bromide ((±)-24): To a solution of (±)-**3** (30 mg, 0.06 mmol) in EtOH (1 mL) at RT, 3-(hydroxymethyl)pyridine (120 μL, 1.24 mmol) was added and the mixture stirred at RT for 29 h and further 67 h at 40 °C. The mixture was evaporated in vacuo and the residue dissolved in MeOH. Precipitation from Et_2O gave (±)-**24** (35 mg, 95 %) as yellow crystals. M.p. 188 °C (decomp); ^{1}H NMR (400 MHz, CD_3OD): δ = 1.80–1.94 (m, 2H, H-C(7), H-C(8)), 2.10–2.21 (m, 2H, H-C(7), H-C(8)), 2.23–2.30 (m, 2H, $^+NCH_2CH_2$), 2.87 (ddd, J = 12.5, 8.2, 4.3 Hz, 1H, H-C(6)), 3.00 (ddd, J = 12.5, 8.6, 6.9 Hz, 1H, H-C(6)), 3.46–3.61 (m, 3H, H-C(8b), $^+NCH_2CH_2CH_2$), 3.79 (ddd, J = 9.1, 7.3, 1.6 Hz, 1H, H-C(8a)), 3.88 (t, J = 8.5 Hz, 1H, H-C(3a)), 4.45 (d, J = 8.7 Hz, 1H, H-C(4)), 4.63 (td, J = 7.6, 1.2 Hz, 2H, $^+NCH_2$), 4.84 (s, 2H, CH_2OH), 6.62 (s, 1H, Ar), 7.09 (d, J = 4.0 Hz, 1H, Ar), 7.40 (d, J = 4.0 Hz, 1H, Ar), 8.07 (dd, J = 8.0, 6.1 Hz, 1H, pyridinium), 8.55 (d, J = 8.1 Hz, 1H, pyridinium), 8.92 (d, J = 6.1 Hz, 1H, pyridinium), 8.99 ppm (s, 1H, pyridinium); ^{13}C NMR (100 MHz, CD_3OD): δ = 24.2, 30.4, 30.6, 36.4, 50.8, 52.4, 60.4, 61.1, 62.6, 69.5, 101.2, 128.1, 128.9, 129.0, 134.1, 143.9, 144.5, 144.6, 145.5, 164.9, 165.0, 177.5, 180.0 ppm (2 C not visible); IR (ATR): $\tilde{\nu}$ = 3303, 3021, 2950, 2868, 1769, 1699, 1612, 1474, 1427, 1397, 1344, 1297, 1207, 1173, 1065, 998, 920, 878, 796, 687 cm^{-1}; HR-MALDI-MS: m/z (%): 515.1337 (43), $[M-Br]^+$, calcd for $C_{25}H_{26}{}^{37}ClN_4O_4S^+$: 515.1332, 513.1359 (100), $[M-Br]^+$, calcd for $C_{25}H_{26}{}^{35}ClN_4O_4S^+$: 513.1358; elemental analysis calcd (%) for $C_{25}H_{26}BrClN_4O_4S$ (592.05): C 50.56, H 4.41, N 9.43; found: C 50.83, H 4.63, N 9.29.

1-{3-[(3a*SR*,4*RS*,8a*SR*,8b*RS*)-4-[5-(5-Chloro-2-thienyl)-1,2-oxazol-3-yl]-1,3-dioxooctahydrodipyrrolo[1,2-*a*:3′,4′-*c*]pyrrol-2(3*H*)-yl]propyl}-1-(2-hydroxyethyl)pyrrolidinium bromide ((±)-25): To a solution of (±)-**3** (20 mg, 0.041 mmol) in EtOH (1 mL) at RT, *N*-(2-hydroxyethyl)pyrrolidine (97 μL, 0.825 mmol) was added. The mixture was stirred at RT for 17 h, at 40 °C for four days, and evaporated to dryness. The residue was dissolved in MeOH. Precipitation from Et_2O gave (±)-**25** (3 mg, 12 %) as colorless crystals. M.p. 182 °C; ^{1}H NMR (600 MHz, $CDCl_3$): δ = 1.79–1.90 (m, 2H, H-C(7), H-C(8)), 1.96–2.03 (m, 1H, pyrrolidinium), 2.12–2.25 (m, 5H, H-C(7), H-C(8), $^+NCH_2CH_2CH_2N$, pyrrolidinium), 2.88 (ddd, J = 12.7, 8.3, 4.3 Hz, 1H, H-C(6)), 2.95 (ddd, J = 12.8, 8.9, 7.1 Hz, 1H, H-C(6)), 3.34–3.76 (m, 9H, H-C(8a), H-C(8b), $^+NCH_2CH_2CH_2N$, $^+NCH_2CH_2CH_2N$, pyrrolidinium, CH_2CH_2OH), 3.82 (t, J = 8.4 Hz, 1H, H-C(3a)), 3.87–3.90 (m, 1H, CH_2OH), 4.14–4.17 (m, 1H, CH_2OH), 4.43 (d, J = 8.7 Hz, 1H, H-C(4)), 6.68 (s, 1H, Ar), 7.12 (d, J = 4.0 Hz, 1H, Ar), 7.44 ppm (d, J = 4.0 Hz, 1H, Ar), protons hidden under solvent peak; ^{13}C NMR (150 MHz, $CDCl_3$): δ = 22.5, 22.6, 23.2, 24.1, 30.0, 36.6, 50.1, 50.7, 52.0, 57.3, 59.7, 61.9, 62.7, 64.6, 65.0, 69.5, 101.5, 128.2, 128.9, 129.1, 134.2, 164.5, 165.2, 177.4, 179.7 ppm; IR (ATR): $\tilde{\nu}$ = 3246, 2950, 1764, 1700, 1696, 1607, 1518, 1472, 1430, 1418, 1399, 1366, 1232, 1151, 1182, 1089, 1060, 1026, 995, 953, 922, 868, 811, 789, 671 cm^{-1}; HR-MALDI-MS: m/z (%): 521.1791 (41), $[M-Br]^+$, calcd for $C_{25}H_{32}{}^{37}ClN_4O_4S^+$: 521.1801, 519.1827 (100) $[M-Br]^+$, calcd for $C_{25}H_{32}{}^{35}ClN_4O_4S^+$: 519.1827, 334.2123 18, $[M-C_7H_4BrClNOS]^+$, calcd for $C_{18}H_{28}N_3O_3{}^+$: 334.2125.

Acknowledgements

This work was supported by a grant from the ETH Research Council and by F. Hoffmann-La Roche AG, Basel. We thank David Wechsler and Daniel Zimmerli, Roche Basel, for the enantiomeric resolutions. We are grateful to Pablo Rivera-Fuentes (ETH) for DFT calculations on the free ligands. We thank Moritz Hunkeler and Sandra Kienast (ETH) for their contributions to the syntheses of some of the S1 needles.

[1] K. Padmanabhan, K. P. Padmanabhan, A. Tulinsky, C. H. Park, W. Bode, R. Huber, D. T. Blankenship, A. D. Cardin, W. Kisiel, *J. Mol. Biol.* **1993**, *232*, 947–966.

[2] a) K. Schärer, M. Morgenthaler, R. Paulini, U. Obst-Sander, D. W. Banner, D. Schlatter, J. Benz, M. Stihle, F. Diederich, *Angew. Chem.* **2005**, *117*, 4474–4479; *Angew. Chem. Int. Ed.* **2005**, *44*, 4400–4404; b) L. M. Salonen, C. Bucher, D. W. Banner, W. Haap, J.-L. Mary, J. Benz, O. Kuster, P. Seiler, W. B. Schweizer, F. Diederich, *Angew. Chem.* **2009**, *121*, 825–828; *Angew. Chem. Int. Ed.* **2009**, *48*, 811–814.

[3] a) M. Nazaré, D. W. Will, H. Matter, H. Schreuder, K. Ritter, M. Urmann, M. Essrich, A. Bauer, M. Wagner, J. Czech, M. Lorenz, V. Laux, V. Wehner, *J. Med. Chem.* **2005**, *48*, 4511–4525; b) S. Roehrig, A. Straub, J. Pohlmann, T. Lampe, J. Pernerstorfer, K.-H. Schlemmer, P. Reinemer, E. Perzborn, *J. Med. Chem.* **2005**, *48*, 5900–5908; c) M. Ieko, T. Tarumi, T. Nakabayashi, M. Yoshida, S. Naito, T. Koike, *Front. Biosci.* **2006**, *11*, 232–248; d) L. Anselm, D. W. Banner, J. Benz, K. Groebke Zbinden, J. Himber, H. Hilpert, W. Huber, B. Kuhn, J.-L. Mary, M. B. Otteneder, N. Panday, F. Ricklin, M. Stahl, S. Thomi, W. Haap, *Bioorg. Med. Chem. Lett.* **2010**, *20*, 5313–5319; e) D. J. P. Pinto, J. M. Smallheer, D. L. Cheney, R. M. Knabb, R. R. Wexler, *J. Med. Chem.* **2010**, *53*, 6243–6274; f) Y.-K. Lee, M. R. Player, *Med. Res. Rev.* **2011**, *31*, 202–283; g) E. Perzborn, S. Roehrig, A. Straub, D. Kubitza, F. Misselwitz, *Nat. Rev. Drug Discovery* **2011**, *10*, 61–75; h) A. Straub, S. Roehrig, A. Hillisch, *Angew. Chem.* **2011**, *123*, 4670–4686; *Angew. Chem. Int. Ed.* **2011**, *50*, 4574–4590.

[4] For reviews on cation–π interactions, see: a) J. C. Ma, D. A. Dougherty, *Chem. Rev.* **1997**, *97*, 1303–1324; b) H. A. Lester, M. I. Dibas, D. S. Dahan, J. F. Leite, D. A. Dougherty, *Trends Neurosci.* **2004**, *27*, 329–336; c) E. T. Kool, M. L. Waters, *Nat. Chem. Biol.* **2007**, *3*, 70–73; d) E. A. Meyer, R. K. Castellano, F. Diederich, *Angew. Chem.* **2003**, *115*, 1244–1287; *Angew. Chem. Int. Ed.* **2003**, *42*, 1210–1250; e) L. M. Salonen, M. Ellermann, F. Diederich, *Angew. Chem.* **2011**, *123*, 4908–4944; *Angew. Chem. Int. Ed.* **2011**, *50*, 4808–4842.

[5] a) P. R. Gerber, K. Müller, *J. Comput.-Aided Mol. Des.* **1995**, *9*, 251–268; b) Gerber Molecular Design, http://www.moloc.ch.

[6] a) U. Obst, P. Betschmann, C. Lerner, P. Seiler, F. Diederich, V. Gramlich, L. Weber, D. W. Banner, P. Schönholzer, *Helv. Chim. Acta* **2000**, *83*, 855–909; b) E. Schweizer, A. Hoffmann-Röder, K. Schärer, J. A. Olsen, C. Fäh, P. Seiler, U. Obst-Sander, B. Wagner, M. Kansy, F. Diederich, *ChemMedChem* **2006**, *1*, 611–621.

[7] L. Anselm, K. Groebke Zbinden, W. Haap, J. Himber, C. M. Stahl, S. Thomi, US 2005/0215599, **2005**.

[8] K. Hilpert, J. Ackermann, D. W. Banner, A. Gast, K. Gubernator, P. Hadváry, L. Labler, K. Müller, G. Schmid, T. B. Tschopp, H. van de Waterbeemd, *J. Med. Chem.* **1994**, *37*, 3889–3901.

[9] a) A. Shivanyuk, J. C. Friese, S. Döring, J. Rebek, Jr., *J. Org. Chem.* **2003**, *68*, 6489–6496; b) N. K. Beyeh, A. Valkonen, K. Rissanen, *Supramol. Chem.* **2009**, *21*, 142–148.

[10] a) S. Bartoli, S. Roelens, *J. Am. Chem. Soc.* **1999**, *121*, 11908–11909; b) S. Bartoli, S. Roelens, *J. Am. Chem. Soc.* **2002**, *124*, 8307–8315; c) C. A. Hunter, C. M. R. Low, C. Rotger, J. G. Vinter, C. Zonta, *Proc. Natl. Acad. Sci. USA* **2002**, *99*, 4873–4876; d) C. A. Hunter, C. M. R. Low, C. Rotger, J. G. Vinter, C. Zonta, *Chem. Commun.* **2003**, 834–835; e) P. Sarri, F. Venturi, F. Cuda, S. Roelens, *J. Org. Chem.* **2004**, *69*, 3654–3661.

[11] a) M. Hendlich, A. Bergner, J. Günther, G. Klebe, *J. Mol. Biol.* **2003**, *326*, 607–620; b) J. Günther, A. Bergner, M. Hendlich, G. Klebe, *J. Mol. Biol.* **2003**, *326*, 621–636.

[12] H. Matter, M. Nazaré, S. Güssregen, D. W. Will, H. Schreuder, A. Bauer, M. Urmann, K. Ritter, M. Wagner, V. Wehner, *Angew. Chem.* **2009**, *121*, 2955–2960; *Angew. Chem. Int. Ed.* **2009**, *48*, 2911–2916.

[13] R. Paulini, K. Müller, F. Diederich, *Angew. Chem.* **2005**, *117*, 1820–1839; *Angew. Chem. Int. Ed.* **2005**, *44*, 1788–1805.

[14] For a similarly positioned conserved water molecule in co-crystal structures of phenylamidinium ligands bound to factor Xa, see: S. Maignan, J.-P. Guilloteau, S. Pouzieux, Y. M. Choi-Sledeski, M. R. Becker, S. I. Klein, W. R. Ewing, H. W. Pauls, A. P. Spada, V. Mikol, *J. Med. Chem.* **2000**, *43*, 3226–3232.

[15] For a similar proposal, see: a) S. Maignan, J.-P. Guilloteau, Y. M. Choi-Sledski, M. R. Becker, W. R. Ewing, H. W. Pauls, A. P. Spada, V. Mikol, *J. Med. Chem.* **2003**, *46*, 685–690; b) M. Nazaré, H.

Matter, O. Klinger, F. Al-Obeidi, H. Schreuder, G. Zoller, J. Czech, M. Lorenz, A. Dudda, A. Peyman, H. P. Nester, M. Urmann, A. Bauer, V. Laux, V. Wehner, D. W. Will, *Bioorg. Med. Chem. Lett.* **2004**, *14*, 2801–2805; c) M. Nazaré, M. Essrich, D. W. Will, H. Matter, K. Ritter, M. Urmann, A. Bauer, H. Schreuder, J. Czech, M. Lorenz, V. Laux, V. Wehner, *Bioorg. Med. Chem. Lett.* **2004**, *14*, 4197–4201; d) J. T. Kohrt, C. F. Bigge, J. W. Bryant, A. Casimiro-Garcia, L. Chi, W. L. Cody, T. Dahring, D. A. Dudley, K. J. Filipski, S. Haarer, R. Heemstra, N. Janiczek, L. Narasimhan, J. McClanahan, J. T. Peterson, V. Sahasrabudhe, R. Schaum, C. A. Van Huis, K. M. Welch, E. Zhang, R. J. Leadley, J. J. Edmunds, *Chem. Biol. Drug Des.* **2007**, *70*, 100–112; e) J. X. Qiao, C.-H. Chang, D. L. Cheney, P. E. Morin, G. Z. Wang, S. R. King, T. C. Wang, A. R. Rendina, J. M. Luettgen, R. M. Knabb, R. R. Wexler, P. Y. S. Lam, *Bioorg. Med. Chem. Lett.* **2007**, *17*, 4419–4427; f) Y. Shi, D. Sitkoff, J. Zhang, H. E. Klei, K. Kish, E. C.-K. Liu, K. S. Hartl, S. M. Seiler, M. Chang, C. Huang, S. Youssef, T. E. Steinbacher, W. A. Schumacher, N. Grazier, A. Pudzianowski, A. Apedo, L. Discenza, J. Yanchunas, Jr., P. D. Stein, K. S. Atwal, *J. Med. Chem.* **2008**, *51*, 7541–7551; g) K. Groebke Zbinden, L. Anselm, D. W. Banner, J. Benz, F. Blasco, G. Décoret, J. Himber, B. Kuhn, N. Panday, F. Ricklin, P. Risch, D. Schlatter, M. Stahl, S. Thomi, R. Unger, W. Haap, *Eur. J. Med. Chem.* **2009**, *44*, 2787–2795.

[16] For selected publications, see: a) R. Abel, T. Young, R. Farid, B. J. Berne, R. A. Friesner, *J. Am. Chem. Soc.* **2008**, *130*, 2817–2831; b) P. Ball, *Chem. Rev.* **2008**, *108*, 74–108; c) B. C. Roberts, R. L. Mancera, *J. Chem. Inf. Model.* **2008**, *48*, 397–408; d) N. Huang, B. K. Shoichet, *J. Med. Chem.* **2008**, *51*, 4862–4865; e) H. Yu, S. W. Rick, *J. Am. Chem. Soc.* **2009**, *131*, 6608–6613; f) T. Ritschel, P. C. Kohler, G. Neudert, A. Heine, F. Diederich, G. Klebe, *ChemMedChem* **2009**, *4*, 2012–2023; g) M. Ellermann, R. Jakob-Roetne, C. Lerner, E. Borroni, D. Schlatter, D. Roth, A. Ehler, M. G. Rudolph, F. Diederich, *Angew. Chem.* **2009**, *121*, 9256–9260; *Angew. Chem. Int. Ed.* **2009**, *48*, 9092–9096; h) S. B. A. de Beer, N. P. E. Vermeulen, C. Oostenbrink, *Curr. Top. Med. Chem.* **2010**, *10*, 55–66; i) R. Abel, N. K. Salam, J. Shelley, R. Farid, R. A. Friesner, W. Sherman, *ChemMedChem* **2011**, *6*, 1049–1066; j) S. E. Wong, F. C. Lightstone, *Expert Opin. Drug Discovery* **2011**, *6*, 65–74.

[17] For related investigations, see references [12] and [15a].

[18] K. Müller, C. Faeh, F. Diederich, *Science* **2007**, *317*, 1881–1886.

[19] B. E. Smart, *J. Fluorine Chem.* **2001**, *109*, 3–11.

[20] H. G. Wallnoefer, T. Fox, K. R. Liedl, C. S. Tautermann, *Phys. Chem. Chem. Phys.* **2010**, *12*, 14941–14949.

[21] a) A. D. Hamilton, D. Van Engen, *J. Am. Chem. Soc.* **1987**, *109*, 5035–5036; b) A. V. Muehldorf, D. Van Engen, J. C. Warner, A. D. Hamilton, *J. Am. Chem. Soc.* **1988**, *110*, 6561–6562; c) for a review, see reference [4d].

[22] a) G. R. Desiraju, *Angew. Chem.* **1995**, *107*, 2541–2558; *Angew. Chem. Int. Ed. Engl.Angew. Chem. Int. Ed.* **1995**, *34*, 2311–2327; b) P. Metrangolo, H. Neukirch, T. Pilati, G. Resnati, *Acc. Chem. Res.* **2005**, *38*, 386–395; c) P. Metrangolo, F. Meyer, T. Pilati, G. Resnati, G. Terraneo, *Angew. Chem.* **2008**, *120*, 6206–6220; *Angew. Chem. Int. Ed.* **2008**, *47*, 6114–6127; d) L. A. Hardegger, B. Kuhn, B. Spinnler, L. Anselm, R. Ecabert, M. Stihle, B. Gsell, R. Thoma, J. Diez, J. Benz, J.-M. Plancher, G. Hartmann, D. W. Banner, W. Haap, F. Diederich, *Angew. Chem.* **2011**, *123*, 329–334; *Angew. Chem. Int. Ed.* **2011**, *50*, 314–318.

[23] W. Kabsch, *J. Appl. Crystallogr.* **1993**, *26*, 795–800.

[24] Collaborative Computational Project, Number 4, *Acta Crystallogr. Sect. D* **1994**, *50*, 760–763.

[25] P. Emsley, K. Cowtan, *Acta Crystallogr., Sect. D: Biol. Crystallogr.* **2004**, *60*, 2126–2132.

[26] G. N. Murshudov, A. A. Vagin, E. J. Dodson, *Acta Crystallogr., Sect. D: Biol. Crystallogr.* **1997**, *53*, 240–255.

Received: September 1, 2011
Published online: December 9, 2011

